EFFECTS OF FGF2 AND OXYGEN IN THE BMP4-DRIVEN DIFFERENTIATION OF TROPHOBLAST FROM HUMAN EMBRYONIC STEM CELLS

Padmalaya Das[1], **Toshihiko Ezashi**[1], **Laura C. Schulz**[1], **Suzanne D. Westfall**[1], **Kimberly A. Livingston**[1], and **R. Michael Roberts**[1,2,*]

1 *Department of Animal Sciences, University of Missouri-Columbia, Christopher S. Bond Life Sciences Center, Columbia, MO. 65211*

2 *Department of Biochemistry, University of Missouri-Columbia, Christopher S. Bond Life Sciences Center, Columbia, MO. 65211*

Abstract

Human embryonic stem cells (hESC) differentiate into trophoblast when treated with BMP4. Here we studied the effects of either low (4 % O_2, **L**) or atmospheric O_2 (20% O_2, **A**) in the presence and absence of FGF2 on H1 hESC cultured in presence of BMP4. Differentiation progressed from the periphery towards the center of colonies. It occurred most quickly in the absence of FGF2 and under **A** and was slowest in presence of FGF2 and under **L**. Chorionic gonadotrophin (CG) production required **A** while FGF2 suppressed progesterone synthesis under both **A** and **L**. FGF2 was then omitted while we examined trophoblast markers SSEA-1 and cytokeratin-7 and -8, whose expression also progressed inwards from the periphery of colonies and occurred more rapidly under **A** than **L**. By day 5, most cells outside central islands of Oct4-positive cells were positive for these antigens under both conditions and many also expressed HLA-G, a marker of extra-villous cytotrophoblast. Under **A,** but not **L,** CGα and CGβ became prominent in GATA2-positive, peripherally located, multinucleated cells. In conclusion, BMP4 induced conversion of hESC exclusively towards trophoblast; FGF2 slowed differentiation, while O_2 accelerated this process and promoted syncytiotrophoblast formation.

Keywords

Cytokeratin; Cytotrophoblast; HLA-G; Human chorionic gonadotropin; Progesterone; Syncytiotrophoblast

INTRODUCTION

The formation of the trophectoderm, the outer epithelial layer of the blastocyst, provides the first visual evidence of differentiation and separation of cell lineages during the development of the mammalian embryo. Trophectoderm is the precursor of placental trophoblast, which forms the active interface with the maternal system and is responsible for carrying out many

of the main functions of the placenta, including physical support, immunological protection, exchange of nutrients, gases and waste products, modifying maternal blood vessels, and controlling physiological responses of the mother through the production of hormones and other bioactive factors (Benirschke, 1994). In the human, cells of the trophectoderm fuse to form a syncytium, which produces human chorionic gonadotropin (hCG) and which surrounds the implanting blastocyst (Potgens et al., 2002). In the mature placenta, two main cell lineages are derived from trophectoderm and its proliferating cytotrophoblast descendants of trophectoderm; villous syncytiotrophoblast and extravillous cytotrophoblast (Georgiades et al., 2002). Villous syncytiotrophoblast, which ultimately lines the intervillous space and whose outer surface becomes bathed with maternal blood, is the primary site of physiological exchange between the fetal and maternal systems and is also characterized by production of hCG (Benirschke, 1994) and forms as a result of fusion between mononuclear, villous-associated, cytotrophoblast cells (Georgiades et al., 2002; Malassine and Cronier, 2002). The second lineage derived from trophoblast stem cells is extravillous cytotrophoblast (Bischof and Campana, 2000), which is multilayered and the major invasive component of the placenta. These cells move from the anchoring villi into the maternal endometrium by two routes: through the uterine stroma and via the lumen of maternal arteries and play a variety of functions including the modification of spiral arteries so that they are no longer capable of responding to maternal vasomotor signals (Pijnenborg, 2002). One marker of extravillous trophoblast is the non-classical HLA protein, HLA-G (McMaster et al., 1998; Redman et al., 1984). However, extravillous cytotrophoblast likely consists of several kinds of differentiated end cells, whose phenotypes have been poorly characterized.

Oxygen tension plays a role in the differentiation of trophoblast cells and is probably low during the first trimester of a human pregnancy (Jauniaux et al., 2000). Cytotrophoblasts cultured *in vitro* under low O_2 conditions, which likely mimic the uterine environment of early gestation, continue to proliferate (Genbacev and Miller, 2000; James et al., 2006a). However, under atmospheric O_2, proliferation of cytotrophoblast slows and syncytiotrophoblasts begin to form through cell fusion (Genbacev et al., 1997). It is also clear that extravillous cytotrophoblasts slow their rate of proliferation and differentiate as they encounter higher oxygen (Genbacev et al., 1996; James et al., 2006a).

Until recently the best *in vitro* models to study the development of human placenta have been primary trophoblast cultures and choriocarcinoma-derived trophoblast cell lines, such as JAr or JEG3 (Ringler and Strauss, 1990). However, there are limitations to the use of these models. In particular, each is already committed to the trophoblast lineage and so early lineage decisions cannot be addressed. Trophoblast cells derived from placenta probably reflect the stage in gestation at which they were isolated, while choriocarcinoma cells have the disadvantage of being tumor cells whose place in the trophoblast lineage is not clear. However, a third model has recently become available. Human ESC have been reported to differentiate into trophoblast spontaneously during standard subculture, as evidenced by the production of hCGβ and progesterone (Thomson et al., 1998). A more directed conversion to trophoblast occurs when the cells are cultured in the presence of BMP4 (Xu et al., 2002). Human ESC colonies exposed to BMP4 rapidly up-regulate genes encoding transcription factors known to play roles in placental development, e.g. *GATA2, GATA3, MSX2*, and ultimately express a range of genes associated with differentiated trophoblast, e.g. *CGA*, *CGB*, *MMP9*, *KRT7*, and *IGFBP3*. It has been unclear whether differentiation induced in this manner is unidirectional, i.e., directed entirely towards trophoblast, as the cells also up-regulate genes more typical of endoderm, e.g., ones encoding alpha-fetoprotein, apolipoprotein A4, transthyretin and plasma retinol binding protein, soon after BMP4 exposure (Xu et al., 2002). Moreover, BMP4-treated hESC form patches of cells that contain multiple nuclei within the same cytoplasm that resemble syncytiotrophoblast, although it is unclear whether these structures are homologous to syncytial trophoblast formed in vivo. Thus, although hESC may serve as a model for extraembryonic

tissue development, the validity of the system needs to be tested in more detail. The conversion to trophoblast is also surprising, since the hESC lines used in these studies were derived from the inner cell mass (ICM), i.e. after trophectoderm and its accompanying stem cells had been specified (Thomson et al., 1998). BMP4 was also a curious candidate to employ as an inducer of trophoblast differentiation, as it synergizes with LIF to maintain mouse ESC in a proliferating, pluripotent state (Chambers and Smith, 2004; Suzuki et al., 2006; Ying et al., 2003). In the case of hESC, FGF2 rather than LIF is the crucial factor for sustaining proliferation and pluripotency, possibly through its capacity to antagonize BMP signaling (Xu et al., 2005). Nevertheless, BMP4-driven trophoblast differentiation still occurs when FGF2 is present in the culture medium provided that the BMP concentration is sufficiently high (Xu et al., 2002).

In the present studies we have examined the ability of BMP4, in presence and absence of FGF2, to direct hESC along the trophoblast lineage in greater detail than that described earlier (Xu et al., 2002). In particular, we wished to assess how the spatial organization of differentiation in terms of trophoblast markers progressed within hESC colonies and whether the progression to trophoblast was measurably more rapid in the absence of FGF2. Second, we predicted that the appearance of syncytiotrophoblast would be accelerated at high O_2 tensions, as occurs when primary cultures of cytotrophoblast are allowed to differentiate in vitro (Genbacev et al., 1997). Third, we anticipated that cells with the features of extravillous cytotrophoblast would differentiate within cultures treated with BMP4.

MATERIALS & METHODS

Culture of human ESC

Human H1 (NIH code WA01) and H9 (WA09) ESC purchased from WiCell Research Institute (Madison, WI) were cultured in six-well tissue culture plates (Nunc, Sigma-Aldrich) containing a monolayer of γ-irradiated (8,000 cGy) mouse embryonic fibroblast (MEF) feeder cells. The culture medium [80% DMEM/F12 supplemented with 20% KnockOut serum replacement (Invitrogen)/1 mM l-glutamine/0.1 mM 2-mercaptoethanol/1% nonessential amino acids (Sigma-Aldrich)] was changed daily and supplemented with 4 ng/ml recombinant human FGF2 (Invitrogen). Colonies were dispersed by using 1 mg/ml collagenase IV (Invitrogen) and passaged either 1:4 or 1:6 every 5–7 days. Cultures were maintained under a humidified atmosphere of 4% O_2/5% CO_2/91 % N_2 in a HERAcell® 150 Tri-Gas Cell Culture Incubator (Thermo Electron Corporation) at 37°C (**L**). Alternatively, cultures were maintained under a standard gas atmosphere of humidified air/5% CO_2 (**A**). For feeder-free cultures, plates were coated with poly-D-lysine plus Matrigel® (Becton Dickinson) diluted 1:30 in DMEM/F12 (Invitrogen), and the cells were grown in medium conditioned by MEF (Xu et al., 2001). To study the effects of FGF2, recombinant human BMP4 (R&D Systems) was added at a fixed concentration (10 ng/ml) either in its presence or absence from the second day of culture after passage for up to eight additional days.

Morphometry

hESC colonies were photographed under a Leica MZFLIII stereo microscope or on an Olympus CKX41 inverted microscope. Areas of total colonies and differentiated areas within colonies were calculated from digital images of multiple colonies by using the MetaMorph imaging system (Universal Imaging, Downingtown, PA). Two-way comparisons, e.g., **A** vs. **L**, were analyzed by an unpaired *t* test (prism 4, GraphPad, San Diego). For multiple comparisons, data were analyzed by one-way ANOVA followed by Tukey's multiple comparison test to compare selected pairs of experimental groups. Data are presented as the mean ± SEM in μm^2. Differences of $P < 0.05$ were considered significant.

Immunofluorescence Microscopy

hESC colonies were grown on coverslips coated with poly-D-lysine plus Matrigel and placed in six-well tissue culture plates. After fixation in a 4% paraformaldehyde/PBS solution for 15 min and permeabilization in 1.0% Triton X-100/PBS for 30 min, blocking against non-specific ligands was performed with 5% goat serum plus 5% BSA in PBS for about 1–2 h. Where paraformaldehyde fixation negatively affected antigenicity of the candidate protein under study, fixation was performed in either methanol or acetone for 20 min at room temperature, followed by three washes with PBS. The primary antibodies and their source are described in Supplemental Table 1. After fixation, coverslips with attached colonies of hESC were incubated with appropriately diluted serological reagent for either 2–4 h at room temperature or overnight at 4°C. Secondary antibody staining was performed with either Alexa Fluor 568 or 488-labeled detection reagents (goat anti-rabbit, goat anti-mouse, goat anti-rat antibodies; Molecular Probes) at a 1:500 dilution. Nuclei were labeled with TO-PRO-3 (Molecular Probes). Coverslips were viewed either by epifluorescence under the 4x objective of an Olympus Provis AX-70 inverted microscope with a U-MBC multi-control box (Melville, NY, USA) equipped with a cooled charge-coupled device camera (Photometrics CoolSnap-ES, Tucson, TX, USA) or by confocal microscopy (see below). Controls were performed with the omission of primary antibodies in all the experiments performed with epifluorescence and confocal microscopy (see below) (Supplemetary Figure 2).

Confocal microscopy

Some initial images were captured by using a Radiance 2000 confocal system (Bio-Rad) coupled with an Olympus IX70 microscope. The majority of the confocal studies were conducted on a Zeiss META NLO two photon confocal system (Carl Zeiss, Obercohen, Germany) with a Zeiss Axiovert 200M microscope. Green or red fluorescence from the Alexa Fluor-conjugated second antibodies were imaged by using 10x or 20x Universal Plan Apochromat objectives under the 488 or 568 nm excitation wavelengths of a Kr/Ar mixed gas laser, a 488 nm Ar laser (green) and a 543 HeNe laser (red). The 637 nm excitation line of a Red-Diode laser was used to detect nuclei stained with TO-PRO-3 iodide. All images were obtained at 1024×1024 pixel resolution under sequential scan settings. Laser power, gain, and optimum pinhole levels were kept constant across a given set of samples on which comparisons were being made during a single session at the microscope. Single optical sections through the median planes of colonies were captured with either the Bio-Rad software (Lasersharp 2000 version 5.0 for Windows) or Zeiss LSM software. Optical sections were also obtained at 0.3 μM intervals along the z-axis and cropped by using the LSM software. Images were organized and assembled in Photoshop CS (Abobe Systems, La Jolla, CA). All raw images are available upon request.

Immunoassays

Media collected from hESC were stored at −20°C until assay. hCGβ and progesterone were measured by using solid-phase sandwich ELISA and competitive ELISA kits (catalog #. BQ 047F and BQ 072S from Bio-Quant, San Diego) respectively. Standards were supplied by the manufacturer, and the sensitivities of the assays were 0.53 milliunits/ml and 0.3 ng/ml. For all assays, samples were appropriately diluted to fall within the recommended ranges of the standard curves and assayed in triplicate.

RESULTS

Response of hESC colonies to BMP4 in presence of FGF2

Human ESC differentiate into trophoblast in the presence of BMP4 (Golos et al., 2006; Xu et al., 2002), although it is unclear from these early studies whether other lineages were also

represented in the colonies and the spatial organization of the differentiation pattern. Fig. 1a is a collage hand-assembled from 16 separate confocal images on the BioRad instrument encompassing a large H1 ESC colony that had been immunostained for Oct4 (pink), hCGβ (green), and nuclear material (blue) after growth for ten days in presence of BMP4 (10 ng/ml) and FGF2 (4 ng/ml) under **A** conditions. Fig. 1b represents a digitally assembled collage of an hESC H9 colony imaged under the x10 objective of the Zeiss instrument and stained for hCGαand -β The late stage pattern of differentiation in response to BMP4 observed in Fig. 1a & b is typical for both the H1 and H9 cell lines under **A**. Cells towards the outside of the colonies no longer express Oct4, and Oct4 staining, instead, becomes confined to a central core of densely packed cells (Fig. 1a). Conversely, the expression of hCGβ (Fig. 1a) and the co-expression of hCGα and–β (Fig. 1b) become localized to large, flattened cells that are concentrated on the very periphery of the colony, while a region of Oct4-negative and hCG-negative cells of relatively uniform appearance occupies the remainder of the colony (Fig. 1a). The stronger fluorescence originating from the hCGα subunit tends to dominate the co-localization signal, an observation addressed later in the paper. At this stage, the transition from Oct4-positive to Oct4-negative cells is sharp, with no apparent intermediary zone (Fig. 1a). These conditions (medium containing FGF2 and under **A**) are essentially those employed by Xu et al. (2002), who first reported the ability of BMP4 to drive cells towards trophoblast, but who did not provide any immunohistochemical information on whole colonies. One observation relevant to the data presented in the next section is that hESC colonies cultured on glass coverslips (as in Fig. 1a & b) differentiate in response to BMP4 more slowly than on a plastic substratum. We have no explanation why differentiation is retarded on glass, although it may relate to the thickness of the Matrigel layer or to the presence of the poly-D-lysine coating on the glass.

The effects of O_2 atmosphere in combination with the presence and absence of FGF2 on BMP4-directed differentiation of hESC

A 2×2 factorial design was used to study the effects of the presence and absence of FGF2 under **L** or **A** oxygen atmospheres on the formation of trophoblast from H1 ESC colonies treated with BMP4 (10 ng/ml). We examined only a single, low dose of BMP4 to simplify the experimental design. In addition, the 10 ng/ml concentration of BMP4, when used in absence of FGF2, appeared to be about as effective as 50 ng/ml in driving differentiation of H1 cells. The FGF2 concentration (4 ng/ml) was selected because it is standard for maintenance of pluripotency in hESC cultures (Amit et al., 2000). Colonies were allowed to become established for 24 h on a plastic substratum coated with Matrigel before adding medium containing BMP4. The medium was replaced every 24 h to assess the production of hCGβ and progesterone. Colony size and morphology were examined daily by phase contrast microscopy.

After 24 h of BMP4 treatment, larger cells with a cobblestone appearance became evident around the periphery of the colonies in all four treatment groups (**A** ± FGF2 and **L** ± FGF2), suggesting that morphological differentiation had been initiated (Fig. 2a, d, g, j). With longer culture, the differentiated region, evident by the change in cell morphology, proceeded inwards from the periphery towards the center of the growing colonies, leaving a progressively smaller area of densely packed, small undifferentiated cells, which remained Oct4-positive (Fig. 1a & Supplemental Fig. 1 & 2). The extent of this transition towards morphologically differentiated cells was faster in cultures containing no FGF2 and maintained under **A** (Fig. 2g, h, i) than under the other three conditions. By day 3, these colonies often had transformed more or less completely and were comprised largely of cells with a uniform cobblestone appearance (Fig. 2h), while the central area of presumably pluripotent cells was either small or had disappeared. Differentiation was slowest in the cultures containing FGF2 and under **L** (Fig. 2d, e, f). Even in the absence of FGF2, **L** retarded differentiation and tended to preserve larger areas of undifferentiated cells (Fig. 2j, k, l). Similarly, FGF2 had some ability to protect against

differentiation when O_2 tension was high (Fig. 2a, b, c) although the central region of presumed pluripotent cells was usually fragmented and infiltrated with areas of overtly differentiated cells.

Morphometric analyses were used to determine the ratio of areas occupied by overtly differentiated and undifferentiated cells within H1 ESC colonies grown on Matrigel-coated plastic substratum for five days under the four conditions of culture (Fig. 3a & b). These measurements confirmed the major role played by O_2 in controlling the BMP4-induced differentiation of H1 cells. For example, under **A** and in absence of FGF2, over 99 % of the colony area was populated by overtly differentiated cells by day 5 (Fig. 3b), whereas about one-fifth of the colonies remained undifferentiated under **L** conditions. It would appear that the ability of FGF to protect against differentiation, though visible at earlier days, was not so evident after five days of exposure to BMP4.

Incorporation of bromodeoxyuridine

In order to demonstrate that the outer, differentiating cells as well as the inner pluripotent cells within the BMP4-treated colonies continued to proliferate, cultures were provided with bromodeoxyuridine (BrdU) for 45 min 72 h after introduction of BMP4 in order to label cells progressing through the cell cycle. The colonies were immediately fixed, and incorporated label detected by immunofluorescence (Supplemental Fig. 1a & b). The data show that the overtly differentiating cells located in the peripheral regions of the colonies, as well as the densely packed cells placed more centrally, continued to progress through the cell cycle and presumably to divide.

Production of hCGβ and P4

As shown in Fig. 4a (open bars), H1 ESC produced large amounts of hCGβ when FGF2 was absent and the cultures were under **A**. The hCGβ became detectable on day 4, with a peak in production on day 6, which was followed by a sharp decline and then a rebound. This fall off and subsequent recovery varies in magnitude and timing, but is consistent and has been observed with both H1 and H9 cells. It appears to coincide with the detachment of some clumps of cells from the peripheral regions of the colonies (data not shown). The subsequent rebound of production may be due to further differentiation of cells not previously producing the hormone, but this phenomenon has not been investigated fully. Under **A**, when FGF2 was present in the medium, the production of hCGβ was retarded relative to when FGF2 was absent but still reached a high level by day 8 (Fig. 4a, black bars). BMP4 had little ability to stimulate the production of hCGβ under **L**, particularly in presence of FGF2, with amounts barely registering above background in the assay. Together, these data suggest that the presence of a high O_2 atmosphere, rather than the absence of FGF2, is the predominant driver of hCGβ expression in hESC.

The effects of O_2 and FGF2 on production of progesterone (P4) (Fig. 4b) were somewhat different than those observed for hCGβ. BMP4-induced P4 production was always high in the absence of FGF2 under both **L** and **A** conditions, although this effect was further enhanced under **A.** Only small amounts of P4 were produced in the presence of FGF2, with scarcely any of the steroid detectable under **L**.

Expression of SSEA-1 and cytokeratins

As the absence of FGF2 accelerated BMP4-mediated differentiation of hESC, all subsequent experiments were performed without FGF2 in the medium, and comparisons were only made between **A** and **L**. hESC were cultured on Matrigel-coated coverslips for up to six days after addition of BMP4 and withdrawal of FGF2. In an initial study, H9 ESC colonies were stained with the pluripotent marker, Oct4, and the differentiation marker, SSEA-1, to follow the pattern

of differentiation over time (Fig. 5). As was noted in Fig. 2, colonies differentiated from the periphery towards the center. The nuclei of most cells in the colonies, including those that had acquired a cobblestone appearance, remained Oct4-positive through the first three days after exposure to BMP4. SSEA-1 expression was first noticeable in the outer regions of the colonies on day 3, particularly under **A** (Fig. 5b & e). By day 5, however, all of the overtly differentiated cells outside the central area of Oct4-positive cells expressed Oct4 weakly, if at all, and were SSEA-1-positive (Fig. 5c & f). Some of the smaller colonies had differentiated completely by five days and displayed no evidence for Oct4 expression (data not shown). Although differentiation again appeared to be somewhat accelerated under **A** (Fig. 2 j–l versus g–i), the general pattern of staining under the two conditions by day 5 was quite similar.

The onset of expression of cytokeratin-7, a widely used marker for trophectoderm cells expression, was similarly assessed under **A** and **L** following exposure of hESC to BMP4 (Fig. 6). Results mirrored those for SSEA-1. Staining for cytokeratin-7 was progressive and again was initiated in the periphery of the colonies (Fig. 6b & e). By day 4 under **A**, cytokeratin staining was evident throughout the outer regions of the colony, (Fig. 6f). Day 4 colonies under **L** were similar, but tended to be somewhat delayed compared to colonies under **A** (Fig. 6c). After five days, cytokeratin-7-positive cells were present up to the boundary presented by the central clusters of Oct4-positive cells under both **L** and **A** conditions (Fig. 6g–i). Staining, although cytoplasmic, was concentrated close to the cell membrane, thereby providing a net-like appearance to the colonies when viewed under high magnification (Fig. 6i). Fluorescence intensity within individual colonies was quite heterogeneous, with some areas appearing much brighter than others. In particular, strands or columns of brightly fluorescent cells could be observed amongst a background of less bright cells (Fig. 6 g & h).

HLA-G localization

Next we examined the localization of HLA-G, a glycoprotein whose expression in humans is believed to be confined largely to placenta, specifically extravillous cytotrophoblast (McMaster et al., 1995). We performed immunostaining to determine if the hESC colonies that had been treated with BMP4 contained HLA-G expressing cells possibly representing the extravillous cytotrophoblast lineage. To do so, we employed the 4H84 monoclonal IgG1 antibody, which is directed against amino acids 61–83 of HLA-G and expected to recognize all isoforms of the antigen and not distinguish among them (McMaster et al., 1998; McMaster et al., 1995). At day 5, HLA-G was expressed under both **A** and **L** (Fig. 7). As with the cytokeratin-7 and SSEA-1 (Figs. 5 & 6), expression was generally much stronger outside the central region of presumed pluripotent cells, although there were regions where HLA-G staining clearly penetrated within the core region (Fig. 7d). Expression outside this region was also extremely heterogeneous. Most cells expressed HLA-G on their margins, presumably as the expected integral plasma membrane glycoprotein (Hunt et al., 2000), and often also in a perinuclear zone (Fig. 7b). Some areas of the colony appeared almost devoid of HLA-G or expressed it very weakly (Fig 7c). Many of the cells with surface label also showed strong cytoplasmic labeling, evident as dots of fluorescence, presumably representing intracellular vesicles (Fig. 7 a & b). Other regions appeared to be organized loosely into columns, and showed intense cytoplasmic staining that fluoresced much more brightly than surrounding regions (Fig. 7c).

Human CGα and –β localization

Human CG production is widely accepted as a marker of trophoblast, especially multinucleated syncytiotrophoblast (Georgiades et al., 2002). Fig. 1a & b shows that hCG expression in H1 and H9 hESC colonies exposed to BMP4 is associated with a peripheral ring of flattened cells that might conceivably represent syncytiotrophoblast. Since hCGβ, but not the α-subunit, is produced by a number of human non-trophoblastic tumors (Stenman et al., 2004) and because

coordinate synthesis of both subunits is required to provide functional hormone, we immunostained ESC colonies that had been cultured in the presence of BMP4 under **A** and **L** for both hCGα and -β (Fig. 8a & e). A zone of cells positive for both subunits was evident at the very periphery of the colony under **A** conditions (Fig. 8a). Where boundaries of colonies merged, hCG-positive areas were often present. No such extensive peripheral labeling was observed after colonies had been grown under **L** (Fig. 8e). All cells that stained positively for hCGβ (red) under both **A** and **L** also stained for hCGα (green), providing evidence of production of functional hormone. However, expression of the α-subunit was more widespread than expression of the β-subunit, with some cells appearing only to express hCGα (Fig. 8b–d & f–h). Presumably, these colonies are producing free α-subunit and not the heterodimeric hormone. Interestingly, flattened cells on the margins of the colonies that were positive for hCGβ often also stained for HLA-G (Fig. 7d).

Confirmation of syncytial trophoblast formation in BMP4-treated hESC

The formation of multinucleated syncytiotrophoblast is believed to occur by cell-cell fusion and is accompanied by a rearrangement of desmosomal proteins and loss of cell-cell borders (Douglas and King, 1990). The immunocytochemical localization of desmosomes has previously been used to provide a convenient indicator of the status of trophoblast morphological differentiation into syncytiotrophoblasts (Douglas and King, 1990). Accordingly, in order to identify whether the cells producing hCGα and -β had formed syncytial structures, immunostaining was performed on colonies cultured under **A** with a monoclonal antibody specific for desmosomes in conjunction with a rabbit polyclonal antibody specific for hCGβ (Fig. 9a). Those areas positive for hCGβ (red) contained many nuclei and an apparently continuous cytoplasm, i.e. there was an absence of desmosome staining (green) within the structures that represented putative syncytium (Fig. 9a). These desmosome-free areas contrasted with neighboring hCGβ-negative cells, which were mononucleate and positive for desmosome antigen around their edges. The syncytial cells stained for both cytokeratin 7 (not shown) and cytokeratin-8 (red) (Fig. 9b & c), but the network pattern of cytokeratin distribution delineating the edges of individual cells, as observed in Fig. 6i, has become lost. These hCG-positive regions also showed intense nuclear staining for the transcription factor GATA2 (green) (Fig. 9c). Together the data suggest that the cells producing hCG are syncytial.

DISCUSSION

Trophoblast first becomes evident as a distinct lineage at the blastocyst stage of mammalian development when trophectoderm separates from the ICM (Johnson and McConnell, 2004). Trophectoderm is the precursor of most of the cell types that comprise the fetal portion of the mature placenta (Cross et al., 2002; Roberts et al., 2004). In the case of the mouse, stem cells capable of forming the main differentiated components of trophoblast have been derived from two sources, namely outgrowths of trophectoderm after blastocysts had been cultured in vitro and proliferating cells of the ectoplacental cone, a structure that forms from polar trophectoderm at the embryonic pole of the blastocyst soon after implantation has been initiated (Oda et al., 2006; Quinn et al., 2006). Pluripotent mouse ESC derived from the ICM fail to form trophoblast derivatives except under exceptional circumstances, for example when the transcription factor Oct4 is deliberately silenced (Hay et al., 2004; Niwa et al., 2000; Velkey and O'Shea, 2003). By contrast hESC differentiate readily to trophoblast after the addition of BMP4 and some of its relatives (Xu et al., 2002), a surprising observation since BMP4 in combination with leukemia inhibitory factor (LIF) supports pluripotency rather than differentiation in mouse ESC through induction of *Id* family gene expression (Ying et al., 2003).

In their initial study, performed under 20 % O_2, i.e. **A,** conditions, Xu et al. (2002) showed that several hESC cell lines responded similarly to BMP4 and that in H1 ESC, the line in which the most detailed studies were performed, seven days of exposure to 100 ng/ml BMP4 (in presence of FGF2) up-regulated several genes associated with trophoblast differentiation. In addition, the cells began to secrete low amounts of hCG (measured as hCGβ), estradiol and progesterone (P4) by day 4 of treatment. That BMP4 was directly responsible for the observed effects was emphasized by the ability of antagonists of BMP4 action, such as Noggin, to counteract the directed differentiation towards trophoblast. Xu et al. (2002) also showed that H1 cells plated at low density tend to fuse to form syncytial-like structures that produce hCGβ. In the present study, we have used this hESC model to follow BMP4-directed trophoblast differentiation over time and two-dimensional space and to demonstrate the crucial role played by O_2 in these events.

BMP4 at 10 ng/ml, which is one-tenth the concentration used by Xu et al.(2002) in the majority of their experiments, begins to have an effect on cell morphology relatively quickly, with some visible changes evident on the margins of the colonies after only 24 h (Fig. 2). A single concentration of BMP4 and FGF2 was chosen to permit the simple 2×2 factorial design. In addition we had noted that in absence of FGF2, 10 ng/ml BMP4 was about as effective as 50 ng/ml in inducing morphological differentiation of the cells over time (data not shown). The presence of FGF2 reduced the response to BMP4, while **A** conditions accelerated the differentiation process. Importantly, **L** conditions, particularly when FGF2 was present, inhibited both hCGβ and progesterone production (Fig. 4). For reasons that are presently unclear, FGF2 was particularly effective in reducing the synthesis of progesterone, with a marked depression of synthesis noticeable even under **A**. We have been unable to locate any description of a similar effect of FGF2, which is commonly used as an additive growth factor to primary cell cultures, to inhibit progesterone production by either trophoblast or ovarian cells. This ability of FGF2 on a background of BMP4 to influence steroid hormone production in hESC and the possibility that a particular cell type is targeted by the growth factor deserves further study. However, in order to avoid the complications incurred by including FGF2, all additional experiments in the present study were conducted without it. These later experiments confirmed that BMP4 initiated differentiation from the periphery inwards, that **A** accelerated the process (Figs. 2, 3, 5 & 6) and that the outer cells of the colonies, at least initially, retained Oct4 expression and continued to divide even after they had acquired the more flattened cobblestone appearance (Supplemental Fig. 1). Whether these Oct4-positive outer cells represent trophoblast stem cells, comparable to those characterized for mouse (Niwa et al., 2000) and whether they are already committed irreversibly to the trophoblast lineage are questions we are beginning to pursue.

The striking patterning of the colonies as they differentiate has features of quorum sensing within microbial cultures and films (Waters and Bassler, 2005), a phenomenon that involves differential perception of environmental in-puts by certain cells within the colony and communication of the information to the rest of the population, presumably by chemical gradients and cell to cell contact. It will be of interest to determine whether all cells in naïve hESC colonies respond to BMP4 when the growth factor is applied, which seems unlikely in view of the patterning observed, or whether sensing is confined to a subpopulation, possibly on the periphery. Precisely how cells act in response to BMP4 is not well understood, although signaling is probably initiated by forming a complex with type A and B receptors, such as Alk3 and Alk6, respectively, and subsequent Smad activation and altered gene transcription. An analysis of receptor type distribution, Smad phosphorylation, and trafficking should allow BMP4-responsive cells to be identifiable within colonies. Recently a peripheral, "fibroblastic" population of cells has been identified in hESC colonies that possess the FGF2 receptor, FGFR1, and respond to FGF2 by producing IGFII, TGFβ, and most likely other growth factors (Bendall et al., 2007). IGFII, in particular, appears to be a major supportive factor for hESC

pluripotency, growth, and survival. Conceivably, an analogous population of cells responsive to BMP4 initiates the inward progression of trophoblast differentiation.

Under both **A** and **L** the majority of the cells outside the remaining islands of Oct4-positive cells express both SSEA-1, and cytokeratin-7 by day 5 (Fig. 5 & 6). SSEA-1 is a carbohydrate epitope that is a general marker for human germ cell tumors and hESC differentiation (Draper et al., 2002;Fenderson et al., 1993), while cytokeratin-7 (Blaschitz et al., 2000;Maldonado-Estrada et al., 2004), as well as cytokeratin-8 (Sasagawa et al., 1986) are commonly used for identifying trophoblast. In the transcriptional profiling analysis of Xu et al. (2002), expression of both cytokeratin-7 and -8 transcripts began to increase after 48 h exposure to BMP4. We have confirmed this observation (data not shown), which is consistent with our immunostaining analysis, assuming that protein expression lags behind a change in gene expression. It is interesting that after five days under both O_2 atmospheres, the SSEA-1 and cytokeratin7-positive cells directly abutted the central core regions of presumed pluripotent cells, now providing a sharp boundary between Oct4-negative and Oct4-positive cells (Fig. 5c, f & 6i). These data taken together suggest that BMP4 initiates trophoblast lineage determination in the face of continued Oct4 protein expression and well before some of the traditional markers for trophoblast are acquired. A detailed analysis of gene expression within sampled cell populations harvested at increasing distances from the peripheries of these colonies at different times after BMP4 addition is likely to provide useful insight into how these initiation events are implemented.

A second trophoblast marker, HLA-G, whose role as a non-classical HLA Class I molecule is believed to provide evidence of "self" to maternal natural killer (NK) cells, thereby avoiding a normal immune response (King et al., 2000), was also highly expressed in the BMP-treated hESC colonies by day 5 (Fig. 7). HLA-G is generally held to be produced by extravillous trophoblast, the invasive component of the human placenta (Copeman et al., 2000; Loke et al., 1997), although the specificity of such localization is not universally accepted. HLA-G may also become up-regulated in certain tumors (Hansel et al., 2005). Consistent with our observations, HLA-G expression has been reported not to be particularly responsive to O_2 conditions when extravillous trophoblast outgrowths are cultured *in vitro* (James et al., 2006b). The highest production of HLA-G in our hESC colonies occurred in strands of cells that exhibited a bright cytoplasmic fluorescence (Fig. 7c). These strands of "bright" cells may be homologous to the columns of cytotrophoblast that penetrate maternal endometrium, particularly in the first trimester of pregnancy, although a more detailed phenotyping will be needed to confirm this hypothesis. HLA-G is known to exist in several secreted and soluble forms through alternative splicing (Hunt et al., 2000; Ulbrecht et al., 2004) and with various degrees of glycosylation and proteolytic processing (McMaster et al., 1998). The bright cytoplasmic label might well represent a secretory form of this glycoprotein or some of the variants HLA-G that fail to leave the endoplasmic reticulum as described by Ulbrecht et al. (2004). It was surprising that the majority of cells outside the central Oct4-positive areas, including cells on the periphery positive for hCGβ, stained for HLA-G at day 5, although in some cases the intensity of the signal was exceedingly weak (Fig 7c & d). The heterogeneity of HLA-G staining suggests that it may not be diagnostic just of cells of the extravillous trophoblast lineage but that it is expressed in a range of trophoblast cell types within the colonies, an inference consistent with the view that some forms of the antigen are ubiquitous in trophoblast subpopulations (Hunt, 2006).

Although hCG is produced in limited quantities by various cytotrophoblast cell types, including choriocarcinoma cells (Ringler and Strauss, 1990), its primary source during pregnancy is syncytiotrophoblast, which is regarded as a terminally differentiated cell type renewed basally by replicating villous cytotrophoblast cells (Guilbert et al., 2002). Multinuclear, syncytial cells form when BMP-treated H1 ESC are plated at low density, under which conditions they appear

to fuse readily (Xu et al., 2002). Others have shown that embryoid bodies can provide a model for studying hCG production (Gerami-Naini et al., 2004), and that hCG-producing cell lines derived from embryoid bodies can differentiate spontaneously to syncytiotrophoblast and other placental cell types when cultured in absence of a feeder layer (Harun et al., 2006). In the present paper we demonstrate that hCG-producing cells become concentrated on the peripheries of BMP-treated colonies cultured under **A** (Fig. 8) even when FGF2 is also present (Fig. 1a & b), but are largely absent under **L**. These hCG-producing, large, flat cells have a continuous cytoplasm (Fig. 9), are cytokeratin-7 and -8 positive, and demonstrate strong nuclear expression of GATA2, a transcription factor that can transactivate the hCGα subunit gene (Steger et al., 1994) and is upregulated during spontaneous syncytial formation by cultured human cytotrophoblasts (Cheng and Handwerger, 2005). All evidence suggests that the cells are homologues of placental syncytiotrophoblast. Evidence from the relative staining patterns of hCGα and –β, and from our microarray data (unpublished data), suggest that the former is expressed more strongly than the latter. A similar lack of coordinated expression of the α-subunit relative to the β-subunit is observed during pregnancy and in choriocarcinoma cells (Roberts and Anthony, 1994) and likely reflects the fact that the transcriptional control mechanisms operating on these genes differ and that the free α-subunit has evolved a function distinct from that of the heterodimeric hormone.

The failure of syncytial cells to form under **L** parallels responses of cytotrophoblast cells isolated from late term placenta when they are placed in culture (Alsat et al., 1996). Such cells under lowered O_2 tensions neither fuse nor up-regulate their hCG production in the manner they do under atmospheric O_2 (Kliman et al., 1986). Low O_2 conditions are believed to predominate within uterine endometrium during the first 10–12 weeks of pregnancy, which coincides with the main period of placental growth and invasion (Burton et al., 1999; James et al., 2006a; James et al., 2006b). Hence, the proportion of sycytiotrophoblast remains limited during the first trimester, while villous cytotrophoblast and invasive extravillous cytotrophoblast continue to proliferate under the relatively hypoxic conditions they encounter (Adelman et al., 2000; Caniggia, 2000; Genbacev et al., 1996; Genbacev et al., 1997). Trophoblast cells presumably have precise O_2 sensing mechanisms that play a central role in controlling their behavior and ultimately their differentiation.

In conclusion, the hESC model used in these experiments would appear to mimic many of the cellular changes that provide a fully functional placenta in vivo. In particular, the model provides a means for following the molecular processes that accompany initial lineage commitment to trophoblast, the early and late differentiation events as they unfold over time and in two-dimensional space, and the regulatory responses to O_2. The model might also prove useful for studying how maternal factors, such as inflammatory cytokines, released in response to trophoblast invasion might intervene to alter trophoblast gene expression and cellular phenotype.

Supplementary Material

Refer to Web version on PubMed Central for supplementary material.

Acknowledgements

References

Adelman DM, Gertsenstein M, Nagy A, Simon MC, Maltepe E. Placental cell fates are regulated in vivo by HIF-mediated hypoxia responses. Genes Dev 2000;14:3191–203. [PubMed: 11124810]

Alsat E, Wyplosz P, Malassine A, Guibourdenche J, Porquet D, Nessmann C, Evain-Brion D. Hypoxia impairs cell fusion and differentiation process in human cytotrophoblast, in vitro. J Cell Physiol 1996;168:346–53. [PubMed: 8707870]

Amit M, Carpenter MK, Inokuma MS, Chiu CP, Harris CP, Waknitz MA, Itskovitz-Eldor J, Thomson JA. Clonally derived human embryonic stem cell lines maintain pluripotency and proliferative potential for prolonged periods of culture. Dev Biol 2000;227:271–8. [PubMed: 11071754]

Bendall SC, Stewart MH, Menendez P, George D, Vijayaragavan K, Werbowetski-Ogilvie T, Ramos-Mejia V, Rouleau A, Yang J, Bosse M, et al. IGF and FGF cooperatively establish the regulatory stem cell niche of pluripotent human cells in vitro. Nature. 2007

Benirschke K. Anatomical relationship between fetus and mother. Ann N Y Acad Sci 1994;731:9–20. [PubMed: 7944139]

Bischof P, Campana A. Molecular mediators of implantation. Best Practice & Research in Clinical Obstetrics and Gynaecology 2000;14:801.

Blaschitz A, Weiss U, Dohr G, Desoye G. Antibody reaction patterns in first trimester placenta: implications for trophoblast isolation and purity screening. Placenta 2000;21:733–41. [PubMed: 10985978]

Burton GJ, Jauniaux E, Watson AL. Maternal arterial connections to the placental intervillous space during the first trimester of human pregnancy: the Boyd collection revisited. Am J Obstet Gynecol 1999;181:718–24. [PubMed: 10486489]

Caniggia I, Mostachfi H, Winter J, Gassmann M, Lye SJ, Kuliszewski M, Post M. Hypoxia-inducible factor-1 mediates the biological effects of oxygen on human trophoblast differentiation through TGFB3. The Journal of Clinical Investigation 2000;105:577–87. [PubMed: 10712429]

Chambers I, Smith A. Self-renewal of teratocarcinoma and embryonic stem cells. Oncogene 2004;23:7150–60. [PubMed: 15378075]

Cheng YH, Handwerger S. A placenta-specific enhancer of the human syncytin gene. Biol Reprod 2005;73:500–9. [PubMed: 15888734]

Copeman J, Han RN, Caniggia I, McMaster M, Fisher SJ, Cross JC. Posttranscriptional regulation of human leukocyte antigen G during human extravillous cytotrophoblast differentiation. Biol Reprod 2000;62:1543–50. [PubMed: 10819754]

Cross JC, Anson-Cartwright L, Scott IC. Transcription factors underlying the development and endocrine functions of the placenta. Recent Prog Horm Res 2002;57:221–34. [PubMed: 12017545]

Douglas GC, King BF. Differentiation of human trophoblast cells in vitro as revealed by immunocytochemical staining of desmoplakin and nuclei. J Cell Sci 1990;96(Pt 1):131–41. [PubMed: 2165075]

Draper JS, Pigott C, Thomson JA, Andrews PW. Surface antigens of human embryonic stem cells: changes upon differentiation in culture. J Anat 2002;200:249–58. [PubMed: 12033729]

Fenderson BA, Radin N, Andrews PW. Differentiation antigens of human germ cell tumours: distribution of carbohydrate epitopes on glycolipids and glycoproteins analyzed using PDMP, an inhibitor of glycolipid synthesis. Eur Urol 1993;23:30–6. 36–7. [PubMed: 7682952]

Genbacev O, Joslin R, Damsky CH, Polliotti BM, Fisher SJ. Hypoxia alters early gestation human cytotrophoblast differentiation/invasion in vitro and models the placental defects that occur in preeclampsia. J Clin Invest 1996;97:540–50. [PubMed: 8567979]

Genbacev O, Miller RK. Post-implantation differentiation and proliferation of cytotrophoblast cells: in vitro models--a review. Placenta 2000;21(Suppl A):S45–9. [PubMed: 10831121]

Genbacev O, Zhou Y, Ludlow JW, Fisher SJ. Regulation of human placental development by oxygen tension. Science 1997;277:1669–72. [PubMed: 9287221]

Georgiades P, Ferguson-Smith AC, Burton GJ. Comparative developmental anatomy of the murine and human definitive placentae. Placenta 2002;23:3–19. [PubMed: 11869088]

Gerami-Naini B, Dovzhenko OV, Durning M, Wegner FH, Thomson JA, Golos TG. Trophoblast differentiation in embryoid bodies derived from human embryonic stem cells. Endocrinology 2004;145:1517–24. [PubMed: 14684604]

Golos TG, Pollastrini LM, Gerami-Naini B. Human embryonic stem cells as a model for trophoblast differentiation. Semin Reprod Med 2006;24:314–21. [PubMed: 17123226]

Guilbert LJ, Winkler-Lowen B, Sherburne R, Rote NS, Li H, Morrish DW. Preparation and functional characterization of villous cytotrophoblasts free of syncytial fragments. Placenta 2002;23:175–83. [PubMed: 11945084]

Hansel DE, Rahman A, Wilentz RE, Shih Ie M, McMaster MT, Yeo CJ, Maitra A. HLA-G upregulation in pre-malignant and malignant lesions of the gastrointestinal tract. Int J Gastrointest Cancer 2005;35:15–23. [PubMed: 15722570]

Harun R, Ruban L, Matin M, Draper J, Jenkins NM, Liew GC, Andrews PW, Li TC, Laird SM, Moore HD. Cytotrophoblast stem cell lines derived from human embryonic stem cells and their capacity to mimic invasive implantation events. Hum Reprod 2006;21:1349–58. [PubMed: 16478759]

Hay DC, Sutherland L, Clark J, Burdon T. Oct-4 knockdown induces similar patterns of endoderm and trophoblast differentiation markers in human and mouse embryonic stem cells. Stem Cells 2004;22:225–35. [PubMed: 14990861]

Hunt JS. Stranger in a strange land. Immunol Rev 2006;213:36–47. [PubMed: 16972895]

Hunt JS, Petroff MG, Morales P, Sedlmayr P, Geraghty DE, Ober C. HLA-G in reproduction: studies on the maternal-fetal interface. Hum Immunol 2000;61:1113–7. [PubMed: 11137215]

James JL, Stone PR, Chamley LW. The effects of oxygen concentration and gestational age on extravillous trophoblast outgrowth in a human first trimester villous explant model. Hum Reprod 2006a;21:2699–705. [PubMed: 16807282]

James JL, Stone PR, Chamley LW. The regulation of trophoblast differentiation by oxygen in the first trimester of pregnancy. Hum Reprod Update 2006b;12:137–44. [PubMed: 16234296]

Jauniaux E, Watson AL, Hempstock J, Bao YP, Skepper JN, Burton GJ. Onset of maternal arterial blood flow and placental oxidative stress. A possible factor in human early pregnancy failure. Am J Pathol 2000;157:2111–22. [PubMed: 11106583]

Johnson MH, McConnell JM. Lineage allocation and cell polarity during mouse embryogenesis. Semin Cell Dev Biol 2004;15:583–97. [PubMed: 15271304]

King A, Hiby SE, Gardner L, Joseph S, Bowen JM, Verma S, Burrows TD, Loke YW. Recognition of trophoblast HLA class I molecules by decidual NK cell receptors--a review. Placenta 2000;21(Suppl A):S81–5. [PubMed: 10831129]

Kliman HJ, Nestler JE, Sermasi E, Sanger JM, Strauss JF 3rd. Purification, characterization, and in vitro differentiation of cytotrophoblasts from human term placentae. Endocrinology 1986;118:1567–82. [PubMed: 3512258]

Loke YW, King A, Burrows T, Gardner L, Bowen M, Hiby S, Howlett S, Holmes N, Jacobs D. Evaluation of trophoblast HLA-G antigen with a specific monoclonal antibody. Tissue Antigens 1997;50:135–46. [PubMed: 9271823]

Malassine A, Cronier L. Hormones and human trophoblast differentiation: a review. Endocrine 2002;19:3–11. [PubMed: 12583598]

Maldonado-Estrada J, Menu E, Roques P, Barre-Sinoussi F, Chaouat G. Evaluation of Cytokeratin 7 as an accurate intracellular marker with which to assess the purity of human placental villous trophoblast cells by flow cytometry. J Immunol Methods 2004;286:21–34. [PubMed: 15087219]

McMaster M, Zhou Y, Shorter S, Kapasi K, Geraghty D, Lim KH, Fisher S. HLA-G isoforms produced by placental cytotrophoblasts and found in amniotic fluid are due to unusual glycosylation. J Immunol 1998;160:5922–8. [PubMed: 9637505]

McMaster MT, Librach CL, Zhou Y, Lim KH, Janatpour MJ, DeMars R, Kovats S, Damsky C, Fisher SJ. Human placental HLA-G expression is restricted to differentiated cytotrophoblasts. J Immunol 1995;154:3771–8. [PubMed: 7706718]

Niwa H, Miyazaki J, Smith AG. Quantitative expression of Oct-3/4 defines differentiation, dedifferentiation or self-renewal of ES cells. Nat Genet 2000;24:372–6. [PubMed: 10742100]

Oda M, Shiota K, Tanaka S. Trophoblast stem cells. Methods Enzymol 2006;419:387–400. [PubMed: 17141063]

Pijnenborg R. Implantation and immunology: maternal inflammatory and immune cellular responses to implantation and trophoblast invasion. Reprod Biomed Online 2002;4(Suppl 3):14–7. [PubMed: 12470559]

Potgens AJ, Schmitz U, Bose P, Versmold A, Kaufmann P, Frank HG. Mechanisms of syncytial fusion: a review. Placenta 2002;23(Suppl A):S107–13. [PubMed: 11978067]

Quinn J, Kunath T, Rossant J. Mouse trophoblast stem cells. Methods Mol Med 2006;121:125–48. [PubMed: 16251740]

Redman CW, McMichael AJ, Stirrat GM, Sunderland CA, Ting A. Class 1 major histocompatibility complex antigens on human extra-villous trophoblast. Immunology 1984;52:457–68. [PubMed: 6204930]

Ringler GE, Strauss JF 3rd. In vitro systems for the study of human placental endocrine function. Endocr Rev 1990;11:105–23. [PubMed: 2180684]

Roberts, R.; Anthony, R. Molecular biology of trophectoderm and placental hormones. San Diego, CA: Academic Press; 1994.

Roberts RM, Ezashi T, Das P. Trophoblast gene expression: Transcription factors in the specification of early trophoblast. Reproductive Biology and Endocrinology 2004;2:47. [PubMed: 15236655]

Sasagawa M, Watanabe S, Ohmomo Y, Honma S, Kanazawa K, Takeuchi S. Reactivity of two monoclonal antibodies (Troma 1 and CAM 5.2) on human tissue sections: analysis of their usefulness as a histological trophoblast marker in normal pregnancy and trophoblastic disease. Int J Gynecol Pathol 1986;5:345–56. [PubMed: 2433238]

Steger DJ, Hecht JH, Mellon PL. GATA-binding proteins regulate the human gonadotropin alpha-subunit gene in the placenta and pituitary gland. Mol Cell Biol 1994;14:5592–602. [PubMed: 7518566]

Stenman UH, Alfthan H, Hotakainen K. Human chorionic gonadotropin in cancer. Clin Biochem 2004;37:549–61. [PubMed: 15234236]

Suzuki A, Raya A, Kawakami Y, Morita M, Matsui T, Nakashima K, Gage FH, Rodriguez-Esteban C, Izpisua Belmonte JC. Nanog binds to Smad1 and blocks bone morphogenetic protein-induced differentiation of embryonic stem cells. Proc Natl Acad Sci U S A 2006;103:10294–9. [PubMed: 16801560]

Thomson JA, Itskovitz-Eldor J, Shapiro SS, Waknitz MA, Swiergiel JJ, Marshall VS, Jones JM. Embryonic stem cell lines derived from human blastocysts. Science 1998;282:1145–7. [PubMed: 9804556]

Ulbrecht M, Maier S, Hofmeister V, Falk CS, Brooks AG, McMaster MT, Weiss EH. Truncated HLA-G isoforms are retained in the endoplasmic reticulum and insufficiently provide HLA-E ligands. Hum Immunol 2004;65:200–8. [PubMed: 15041158]

Velkey JM, O'Shea KS. Oct4 RNA interference induces trophectoderm differentiation in mouse embryonic stem cells. Genesis 2003;37:18–24. [PubMed: 14502573]

Waters CM, Bassler BL. Quorum sensing: cell-to-cell communication in bacteria. Annu Rev Cell Dev Biol 2005;21:319–46. [PubMed: 16212498]

Xu C, Inokuma MS, Denham J, Golds K, Kundu P, Gold JD, Carpenter MK. Feeder-free growth of undifferentiated human embryonic stem cells. Nat Biotechnol 2001;19:971–4. [PubMed: 11581665]

Xu RH, Chen X, Li DS, Li R, Addicks GC, Glennon C, Zwaka TP, Thomson JA. BMP4 initiates human embryonic stem cell differentiation to trophoblast. Nat Biotechnol 2002;20:1261–4. [PubMed: 12426580]

Xu RH, Peck RM, Li DS, Feng X, Ludwig T, Thomson JA. Basic FGF and suppression of BMP signaling sustain undifferentiated proliferation of human ES cells. Nat Methods 2005;2:185–190. [PubMed: 15782187]

Ying QL, Nichols J, Chambers I, Smith A. BMP induction of Id proteins suppresses differentiation and sustains embryonic stem cell self-renewal in collaboration with STAT3. Cell 2003;115:281–92. [PubMed: 14636556]
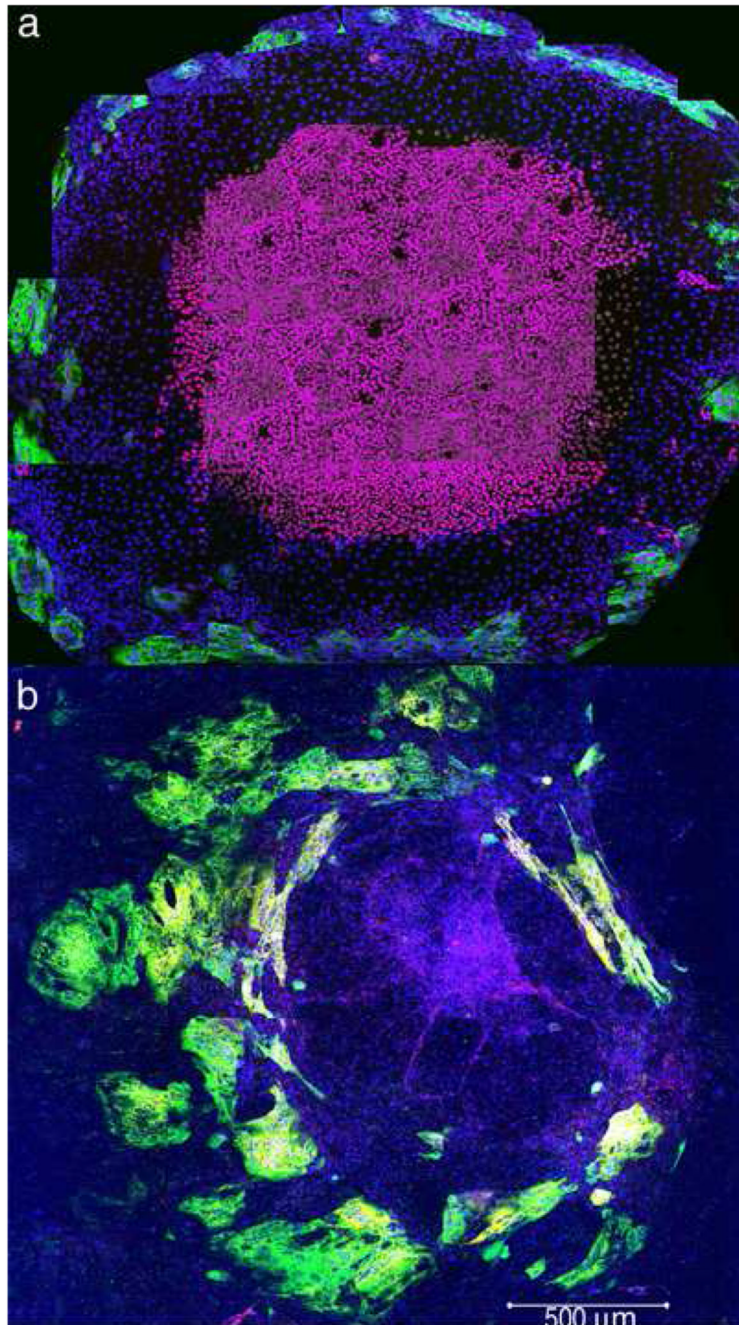
FIGURE 1.
a, Immunostaining of an H1 hESC colony, cultured in the presence of BMP4 and FGF2 for 9 days in atmospheric oxygen, for Oct4 (red) and hCGβ (green). Nuclei have been counterstained with TO-PRO 3 (blue). Twelve photographs were assembled from images acquired from the BioRad confocal system into a collage to visualize the entire colony. Oct4 was selected as a marker of pluripotent cells, while hCGβ is a marker of trophoblast and is associated with flattened areas of cells around the margins of the colonies. BMP4 concentration was 10 ng/ml, FGF2 4 ng/ml. **b**, Co-localization of hCGα (green) and hCGβ (red) in an H9 colony cultured as in Fig. 1**a** above. Regions staining with both antigens appear yellowish-white. Nuclei are stained blue. Some pinkish fluorescence associated with the central core region is non-specific

and is seen on some control samples (not shown) in which the primary anti-hCGβ reagent was omitted. The image is a projection of a tile scanned image assembled by using Zeiss LSM software to visualize the entire colony in the x, y and z planes. The scale bar represents 500 μm.
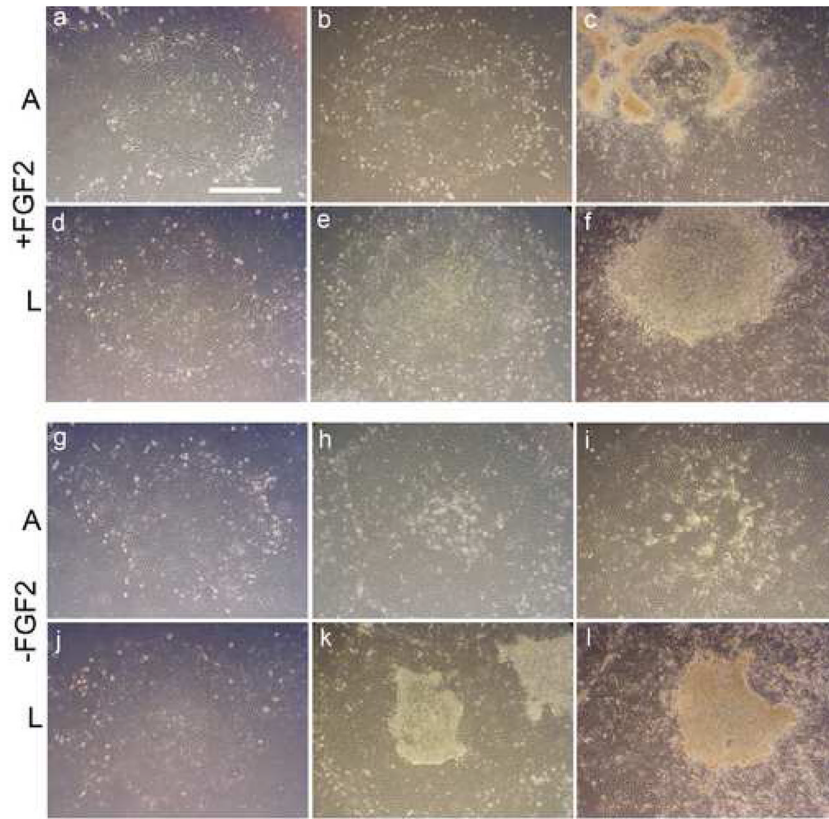
FIGURE 2.
Phase contrast images showing morphology of H1 hESC colonies cultured in the presence of 10ng/ml BMP4 for 1 (**a,d,g,j**), 3 (**b,e,h,k**) or 5 (**c,f,i,l**) days. Cells were cultured in ambient (**A, a–c, g–i**) or low (**L, d–f, j–l**) oxygen, and in the presence (**a–f**) or absence (**g–l**) of FGF2. An area of morphologically differentiated cells, characterized by a cobblestone appearance becomes visible at the periphery of the colony, and progresses inwards under all 4 culture conditions. A central area containing small, presumably undifferentiated cells becomes more densely packed with time in culture. Differentiation was slowest under **L** and FGF2 and most rapid under **A** without FGF2. The scale bar shown in panel **a** represents 1mm.
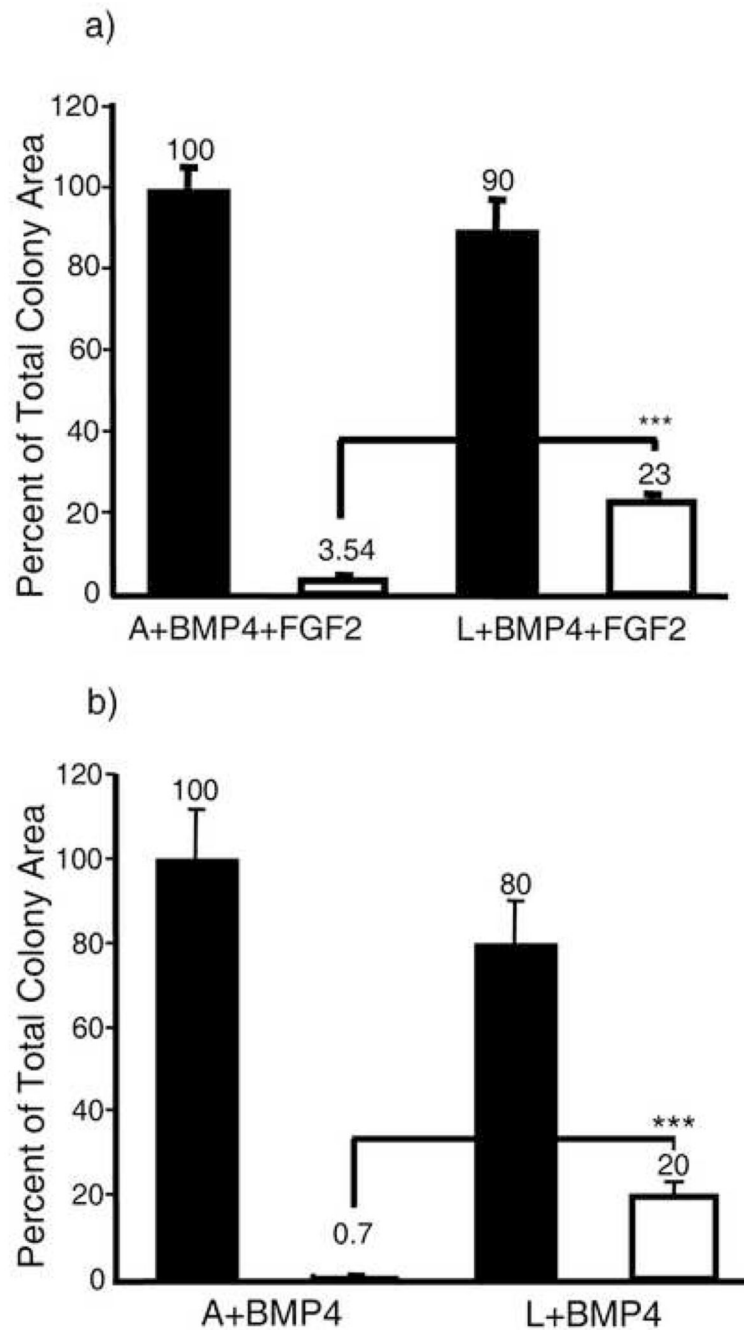
FIGURE 3.
Morphometric analysis of differentiated and undifferentiated areas within H1 hESC colonies after growth for 5 days under either atmospheric (**A**) or low (**L**) oxygen conditions in the presence of BMP4 and FGF2 (**a**) or BMP alone (**b**). Data for each condition were obtained from the analysis of 10 colonies randomly sampled from three independent culture wells of a single experiment. Total colony area (black bars) and the undifferentiated area (open bars) are expressed relative to average total colony area in **A** (100%). [***] $P < 0.0001$.
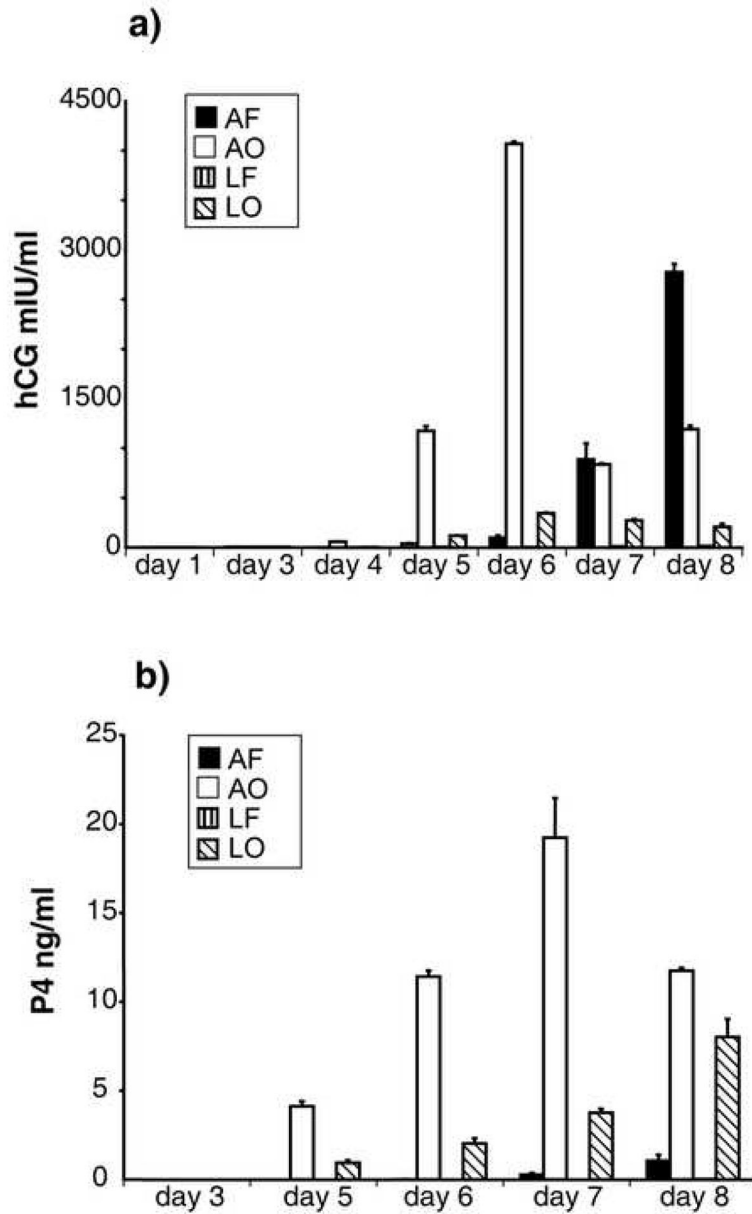
FIGURE 4.
Daily accumulation of hCG (**a**) and progesterone (P4) (**b**) in medium after culturing H1 hESC with BMP4 either in the presence or absence of FGF2 and under either **A** or **L** oxygen conditions. Bars (± SEM) represent cultures exposed to (in order) atmospheric oxygen, FGF2 (AF); atmospheric oxygen, no FGF2 (AO); low oxygen, FGF2 (LF); low oxygen, no FGF2 (LO). Amounts of hCG and P4 released under LF conditions on all days were so low that they were not significantly different from zero. The data represent the results of a single, representative experiment performed on H1 cells. The experiment has been repeated four times, including twice with H9 cells. The peak and subsequent decline in the daily production of hCG on or about day-6 is observed consistently, but varies in magnitude.
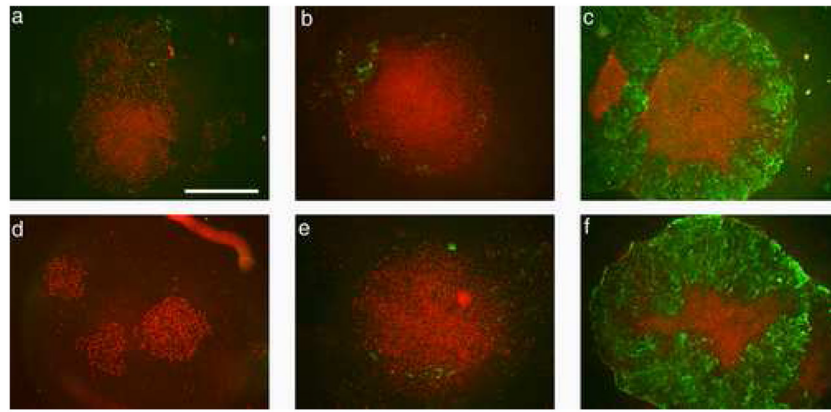
FIGURE 5.
H1 hESC cultured in the presence of BMP4 for 1 (**a, d**), 3 (**b, e**), or 5 days (**c, f**) in either low (**L**) (**a–c**) or atmospheric (**A**) (**d–f**) oxygen immunostained for Oct4 and SSEA-1. By d 5, immunostaining for Oct4 (red) becomes confined to an inner core of densely packed cells, but is still associated with nuclei of most cells in the colonies at d 1 and 3. Note that in **d**, which shows three small colonies, all the cells have apparently responded to BMP4 but all the nuclei remain Oct4-positive. By contrast, staining for the differentiation marker SSEA-1 (green) is initially confined to a few outer cells at d 3 (**b, e**), but becomes associated with all cells outside the dense central core of Oct4-positive cells by d 5 (**c, f**) under both oxygen conditions. Although, not shown, some smaller colonies were entirely SSEA1-positive and Oct4-negative by d 5. Whole colonies were imaged on the Olympus epifluorescence system under a 4x objective. The scale bar in **a** represents 1mm.
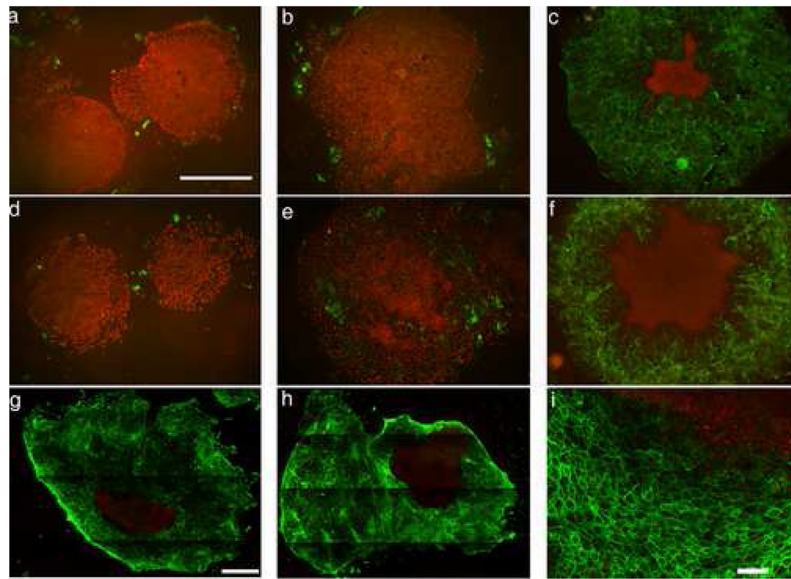
FIGURE 6.
Expression of Oct4 (red) and cytokeratin 7 (green) in H1 (a–f) and H9 (g–i) hESC cultured for in the presence of BMP4. Cells were cultured in either at low (**L**) (**a–c,g**) or atmospheric (**A**) (**d–f, h–i**) oxygen for 1 (**a,d**), 3 (**b,e**), 4 (**c,f**), or 5 (**g–i**) days. By day 5 under both conditions, a central core stains intensely for Oct 4, whereas all cells outside the core are cytokeratin-positive, with intense staining near the cell membrane. The images in **g** and **h** are collages assembled through use of the Zeiss LSM software in order to visualize entire colonies. The scale bar for **g** and **h** represents 500 μm. In the higher power confocal image shown in **i,** the scale bar represents 50 μm. The scale bar represents 1mm in **a–f,** which were photographed on the Olympus epifluorescence system under a 4x objective.
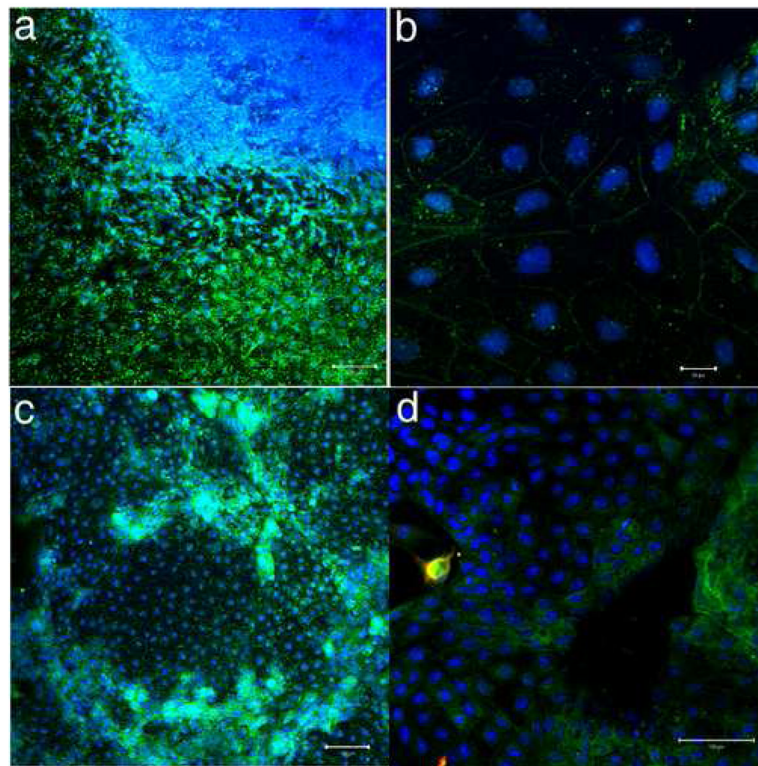
FIGURE 7.
Localization of HLA-G (green) in H9 hESC colonies treated with BMP4 for 5 days under atmospheric (**A**) oxygen. Nuclei are stained with TO-PRO 3 (blue). HLA-G expression was similar under **L** conditions (not shown). HLA-G was variably expressed among cells throughout the differentiated region of the colony, but not in the central core, which can be seen in the upper right-hand corner (**a**). HLA-G is localized to the edges, presumably plasma membrane and within vesicles in perinuclear region of most cells within the differentiated region of the colony (**b**). Some clusters of cells show intense cytoplasmic staining for HLA-G (**c**). In (**d**), the edge of the central core can be seen at right, and the outside edge of the colony at left. Cells which were positive for hCGβ(red) also stained for HLA-G within the cytoplasm, with the double-staining appearing yellow. The scale bars represent 100 μm in **a,c**, and **d** and 20μm in **b**.
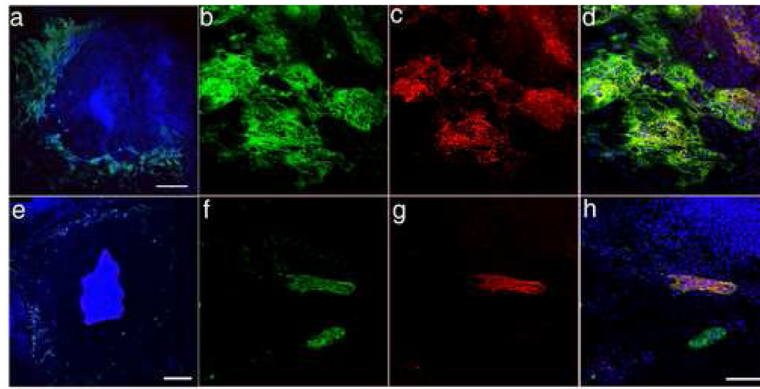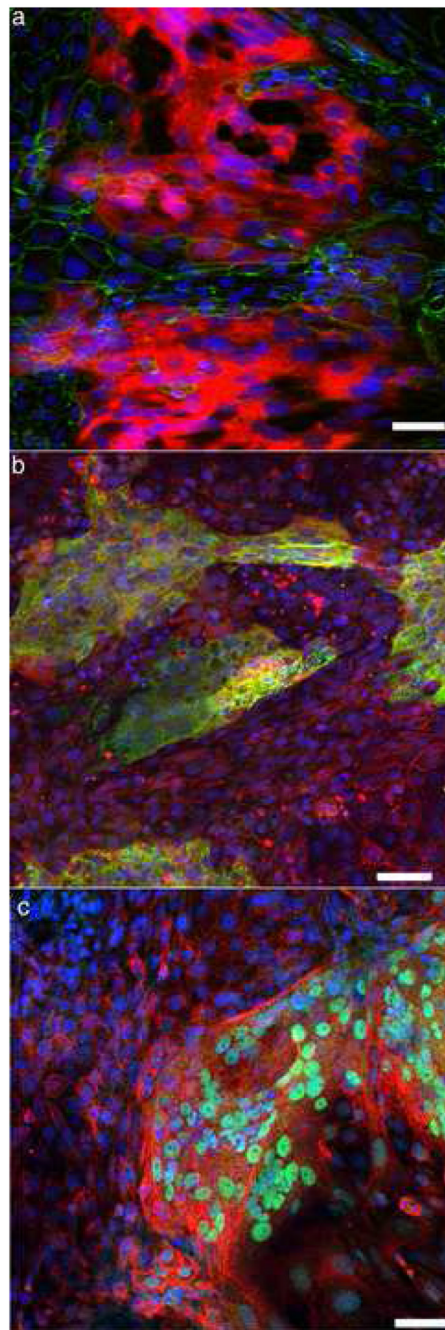
FIGURE 8.
Immunostaining for hCGα (green) and β (red) in H9 hESC colonies cultured under **A** (**a–d**) or **L** (**e–h**) conditions for five days in the presence of BMP4. Nuclei are stained with TO-PRO 3 (blue). The red hCGβ staining was relatively faint compared to the green hCGα, but yellowish color in merged images (**a**, **d**, **e** and **h**) indicate regions of dual expression. Projections of tile scans were used to visualize entire colonies in **a** and **e**, where the scale bar represents 500 μm. Larger areas of hCG-positive cells were present in cells cultured in atmospheric (**A**) compared to low (**L**) oxygen. Higher magnification images show the co-localization of hCGα (**b, f**) and –β (**c, g**) subunits (merged, **d, h**). Note that in **d** and **h** the areas of hCG staining appear to contain many nuclei within a common cytoplasm. All cells positive for hCGβ were also positive for hCGα, but the inverse was not true. The scale bar shown in (**h**) represents 200 μm in **b–d, f–h**.

FIGURE 9.
The presence of syncytial-like structures in H9 hESC cultured in the presence of BMP4 for five days. Nuclei are blue. Images are 3D projections of multiple confocal sections. **a**, H9 cells positive for hCGβ (red) do not have desmosomes (green) separating nuclear areas, suggesting a continuous cytoplasm. **b**, The network of cytokeratin 8 (red) staining that delineates individual cells outside the hCGβ (green) areas is not apparent within areas staining for hCGβ (green). **c**, Syncytial-like regions with continuous cytokeratin 8 staining (red) also show intense nuclear staining for the transcription factor GATA2 (green). Scale bars represent 100 μm.